Broadband processing of West of Shetland data

Rob Telling[1*], Nick Riddalls[1], Ahmad Azmi[1], Sergio Grion[1] and R. Gareth Williams[1] present broadband processing of 2D data in a configuration that enables demultiple algorithms, designed for processing conventional data, to be used as part of a standard prestack time sequence.

The example dataset described here forms part of a 2D broadband well-tie survey conducted within the Shetland-Faroe basin. The water-bottom within the survey area is hard and varies in depth between 120 m and 1700 m. The deeper geology throughout is characterized by a prominent layering of Paleogene flood basalt, varying in thickness from a few hundred metres to over a kilometre. In terms of seismic response, the high impedance contrasts at the water-bottom and at the top of the basalt gives rise to prominent reflections and strong multiples. Additionally, severe attenuation takes place within the alternating layers of basalt and silt and clay stones which limits deeper penetration of energy. It is important for successful imaging to maintain good signal-to-noise ratio below this layer, particularly at the more penetrating low frequencies, and this survey is therefore well suited to a broadband acquisition and processing solution. The high signal-to-noise ratio offered by towing streamers deep below the source of wave noise is important for maximizing the processing bandwidth (Williams and Pollatos, 2012).

A central feature of the processing of this dataset is the use of algorithms designed for processing conventional data, made possible by the adoption of a flat or, as used here, a very mildly slanted streamer configuration during acquisition. In contrast, where strongly slanted or curved profiles are used, algorithms require modification to account for the strong variability of the receiver ghost response with offset (Sablon et al., 2012), due to a breakdown of the stationary wavelet assumption that many processing algorithms require (e.g. semblance velocity analysis, SRME) or alternatively deghosting and re-datuming must be carried out at a much earlier stage in the processing sequence.

Data acquisition

Fifteen 2D lines totalling 2134 km were acquired in May 2013 by *Artemis Atlantic*. The source was an airgun array towed at 8 m depth, with total volume 0.071 m^3 and pressure 141 bar. The shot interval was 25 m. The receiver cable was towed deep with a gentle slant of 1 m per km to facilitate rigging and minimize tug noise. Cable depth was 20 m at the near end and 30 m at the far end. The cable comprised 800 hydrophone channels, the first at an offset of 150 m and with channel spacing of 12.5 m, so 10 km length in total. The filters used were 2 Hz with 18 dB/octave roll-off and 214 Hz with 574 dB per octave roll-off. The main example line shown in this paper was 194 km in length, acquired across the basin sailing in a north-westerly direction. Sea-state varied between 0.5 and 2.5 m wave-heights.

Processing sequence

An outline of the processing sequence is provided in Table 1. The re-datuming was an offset dependent static time shift for gun and cable depth assuming vertical propagation. Source designature included attenuation of bubble energy and zero-phasing for the wavelet and source ghost. Good care was taken throughout processing to ensure the preservation of low-frequency signal content, for example using long (≥ 500 ms) filters and quality checking spectra before and after each process. The low frequency cut-off filter was applied at 2 Hz with 18 dB per octave roll-off. At the upper end, an anti-alias filter was applied prior to resampling to 4 ms, with full amplitude at 112.5 Hz dropping to zero at 124.5 Hz.

1. Re-datum to mean sea-level	8. Offset regularization
2. Source designature	9. F-x deconvolution
3. Anti-alias filter and resample to 4 ms	10. Phase deghosting
4. Swell and linear noise attenuation	11. Kirchhoff prestack time migration
5. Multiple attenuation	12. High-resolution demultiple
6. Anti-alias and alternate channel drop	13. Amplitude deghosting
7. Hi-resolution Radon de-multiple	14. Poststack deconvolution and scaling

***Table 1** Processing sequence.*

[1] *Dolphin Geophysical.*

[*] *Corresponding Author, E-mail: rob.telling@dolphingeo.com*

Swell noise attenuation was carried out in multiple iterations in both common shot and common channel sorts using f-x domain filtering. Linear noise from the direct arrival and tug/tail-buoy noise was attenuated using move-out discrimination after linear Radon transform. An example shot gather before and after noise attenuation is shown in Figure 1 which shows that the signal level is 10-12 dB above the swell noise in the 2-5 Hz band and around 20 dB above the ambient level at the frequency of the first (non-zero) ghost notch. This high signal-to-noise ratio ensures effective deghosting and good final imaging.

Water-layer multiples were prominent in the dataset, in particular those associated with the water bottom and the top of the basalt layer. These key events are marked in Figure 2 as WB and TB respectively together with examples of their respective order of multiples, marked with suffixes M1 and M2. Attenuation of multiples was first carried out using a standard implementation of 2D SRME. Shot interpolation and extrapolation of the near offsets to zero was carried out as a pre-processing step. Figure 2b shows the result for our example line and it can be seen that SRME worked very well in the majority of areas. However, the water column was in the range 120 m to 1150 m and in the shallower regions of the survey, e.g. the yellow box in Figure 2b, there was some residual multiple energy that needed attention. Here, the accuracy of the SRME model was confounded by an incomplete record of the seabed reflection at the near offsets.

We therefore investigated additional multiple models and also tau-p deconvolution, here with a gap (100 ms) chosen long enough to preserve the ghost. The first model was produced using a wave-field extrapolation-based multiple attenuation (WEMA) algorithm, which complemented the SRME result for the multiples associated with the deeper horizons and the second was generated using a shallow-water multiple elimination (SWME) algorithm. Shallow water demultiple is discussed, for example, in Biersteker (2001) and Hargreaves (2006). The results of these tests are shown in Figure 3.

In all cases, the multiple model is adaptively subtracted from the original data with careful attention paid to preserving primary signal while maximizing multiple removal. In the shallow region, a much improved result over SRME alone was found after a second stage of subtraction using a multiple model derived from wave-field extrapolation, Figure 3c. Very similar performance was also obtained by applying tau-p deconvolution (not shown). However, in both cases some residual water-bottom multiple remains. Further tests showed that it was possible to obtain an improved result by applying the shallow water algorithm alone, instead of SRME, Figure 3d. SWME was found to be more effective at removing the first and second order multiples from the water-bottom and beneath the central belt of basalt. The simpler methodology and improved result favour this choice of algorithm, at least in the shallow part of the dataset.

Retaining the ghost during demultiple, particularly SRME and SWME, in principle violates the stationary wavelet assumption, as primaries and their ghosts from two different offsets are combined to predict a multiple with a

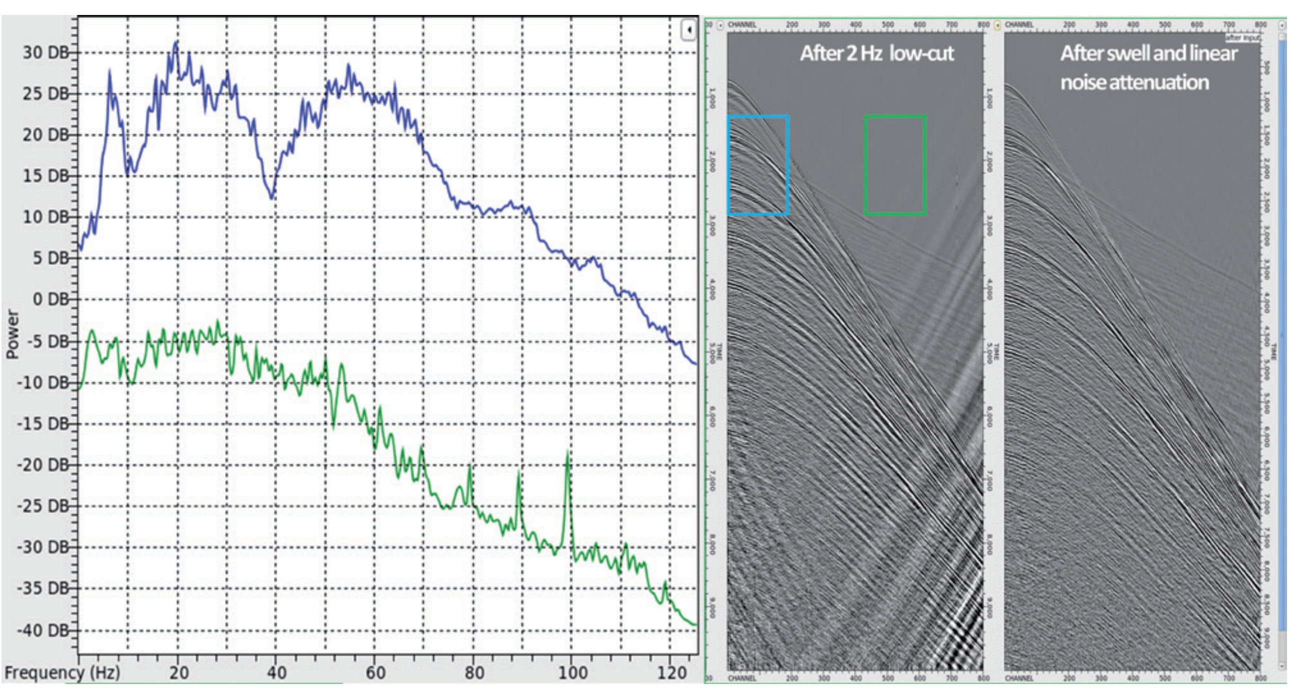

Figure 1 Example shot gathers showing signal plus noise and noise spectra.

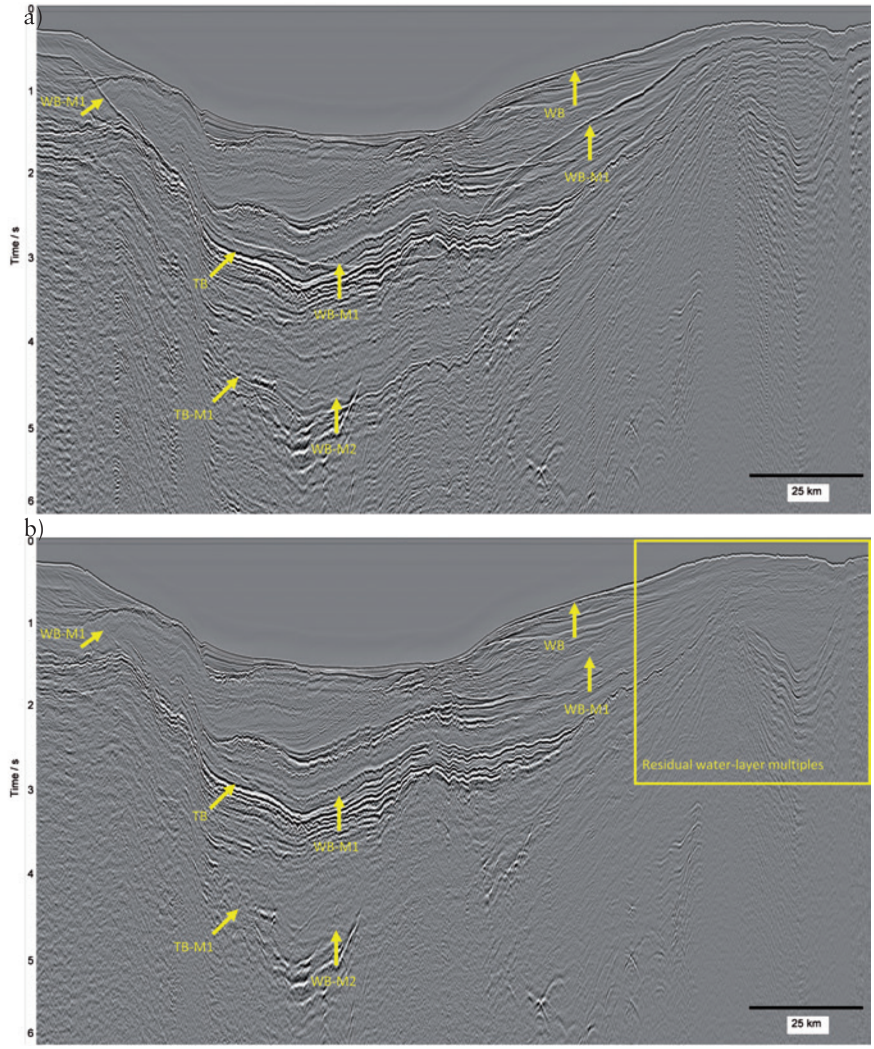

Figure 2 *Stacked section before and after application of 2D SRME which shows generally very effective attenuation of multiple energy. WB = water-bottom, TB = top of basalt, M#=multiple, nth order. However, note that there is residual surface multiple energy corresponding to the TB horizon at the right-hand-side of the section, outlined with the yellow box.*

different offset, and this of course can lead to mismatching of input data and model, and ultimately to ghost distortion. This will particularly be the case for a slanted streamer where there is strong variability of the ghost response with offset. Aware of these concerns, we checked common offset gathers of input data with multiples and of the corresponding SRME multiple model, see Figure 4. Inspection of these gathers indicates that for the acquisition configuration chosen, any such distortions are small and can be corrected for in the least-squares adaptive stage. This then gives the flexibility to deghost at a later stage in the processing with higher signal-to-noise ratio. Initial velocity analysis was conducted at 1 km intervals. Residual multiple attenuation was carried out in two applications of high-resolution parabolic Radon transform. A conservative mute was applied with the initial velocities and then a more discriminating mute after migration velocity analysis to separate primary from multiple based on residual move-out. Residual noise attenuation was carried before migration out on common offset gathers by deconvolution in the f-x domain. Binned offsets were migrated using a 2D Kirchhoff prestack time migration algorithm with 6 km aperture and 50 degree dip limit.

Deghosting comprised a deterministic phase-correction using a priori information on cable depth, water velocity and a sea-surface reflection coefficient, followed by an adaptive amplitude correction. The phase correction was applied before migration on shot gathers transformed to the tau-p domain. This enabled us to account for the changes in delay time of the ghost as a function of arrival angle and proved to be more effective than a phase correction applied post-migration. On the other hand, adaptive amplitude deghosting was carried out after migration on common offset sections for ease of quality control, having verified that this stage was equally successful when applied before or after imaging. The receiver and source ghost notches induced by sea-surface reflections were compensated for using time-space variant deghosting operators, derived

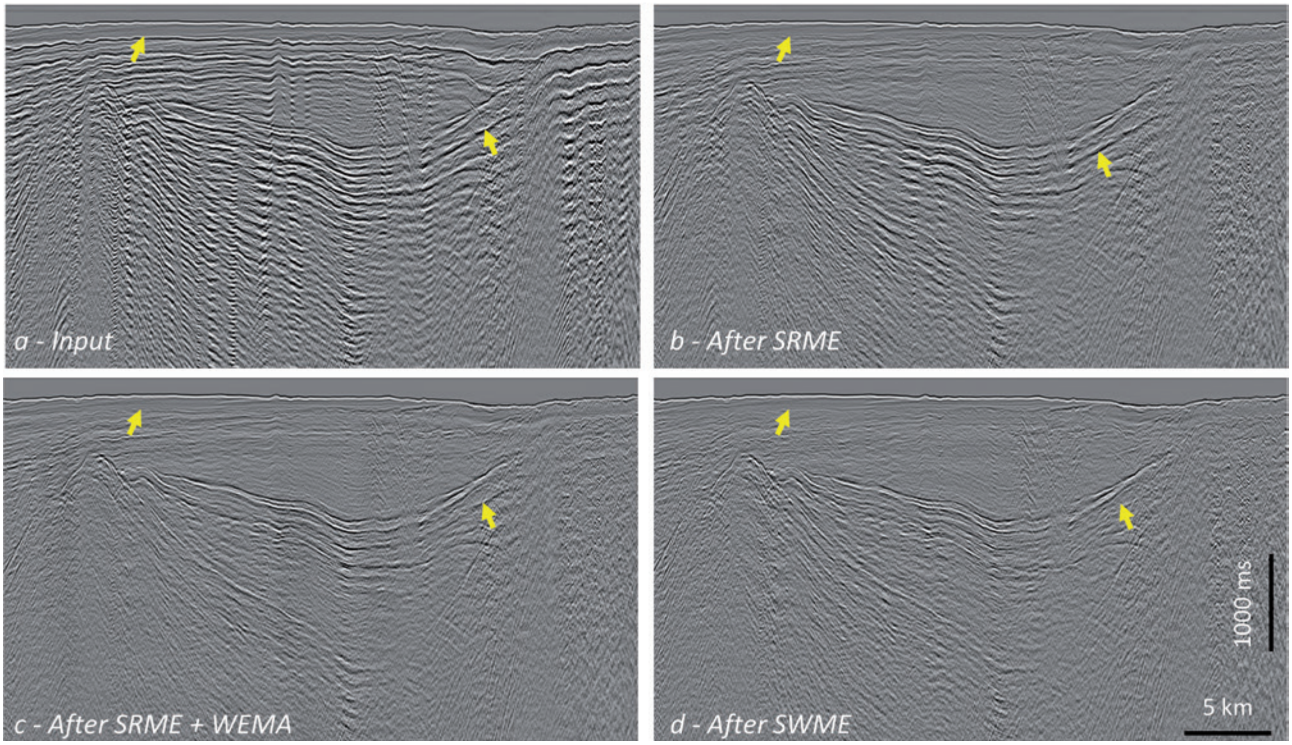

Figure 3 Stacked section for 0-4 seconds, showing zoomed and additionally gained section after Figure 2. a is input before multiple attenuation, b is after SRME, c is after SRME and wave-field extrapolation demultiple and finally, d is after the shallow water demultiple. Yellow arrows indicate positions of first order water-layer mulitples from the water-bottom and from the top of the basalt.

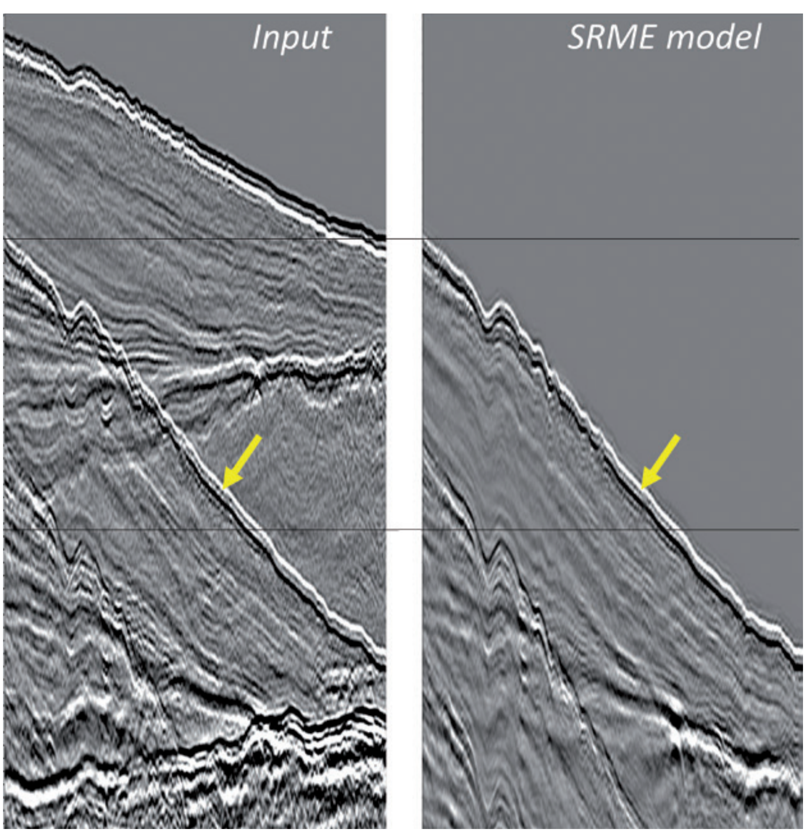

Figure 4 Common offset gather 150 m, showing input data and multiple model after least-squares adaption. Horizontal grid spacing is 500 ms.

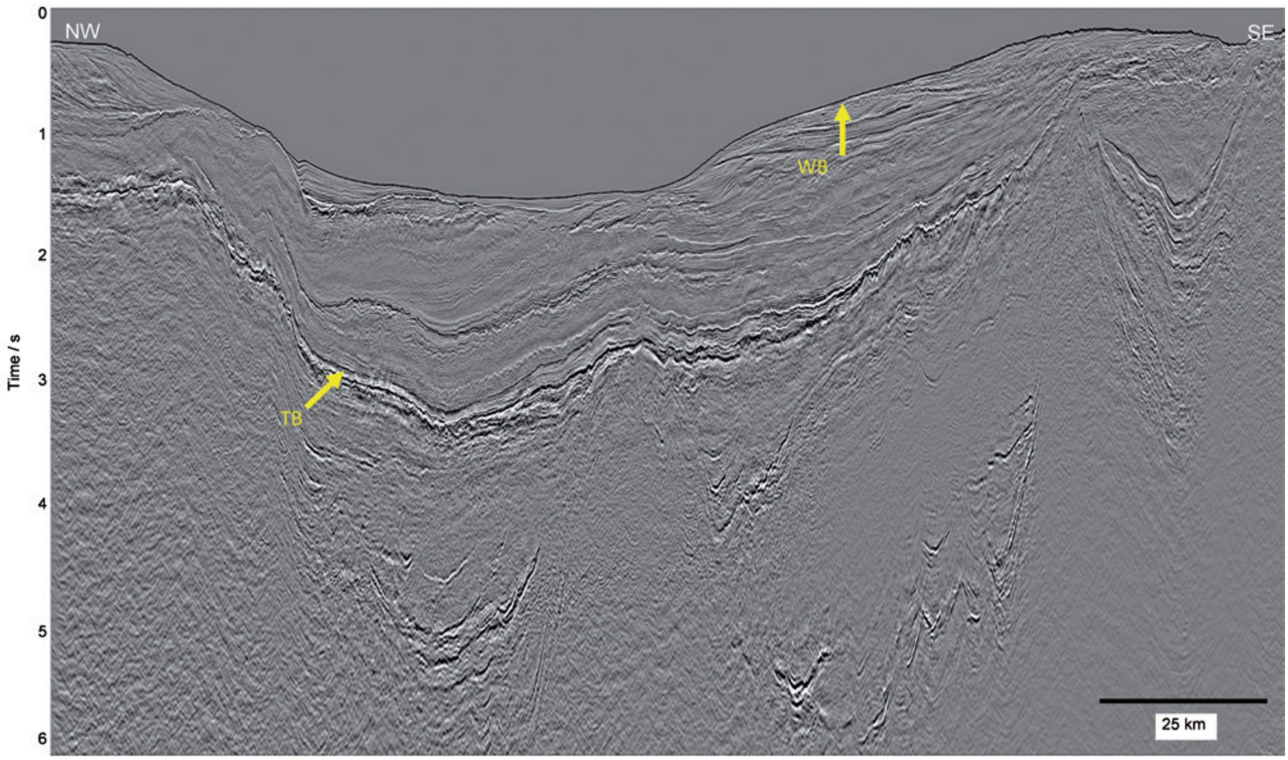

Figure 5 *Final time-migrated, stacked data for the 194 km example line.*

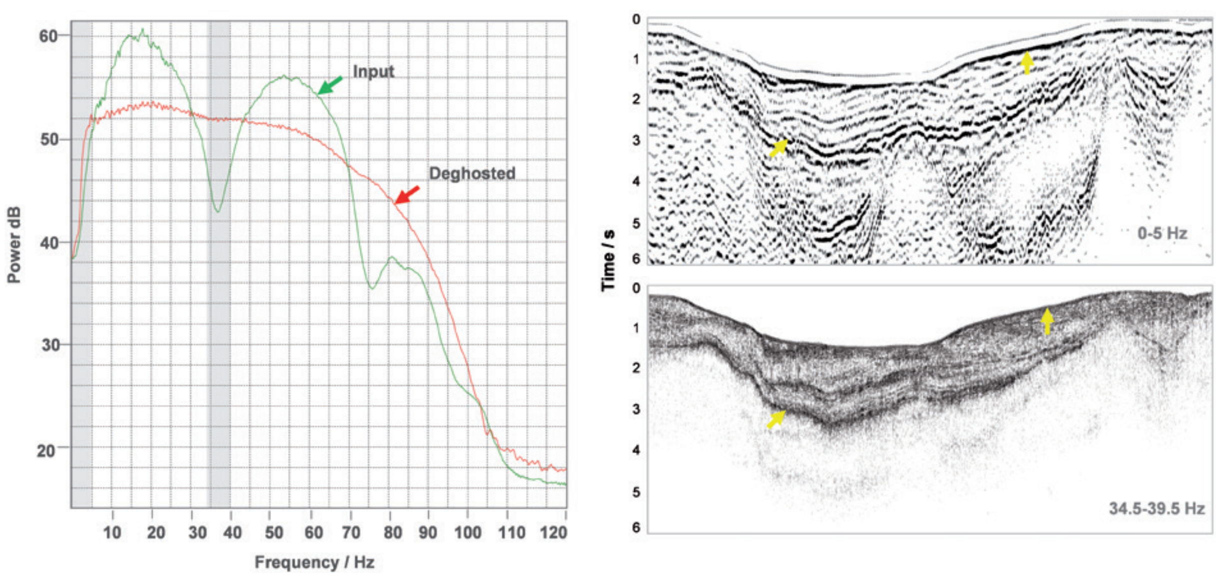

Figure 6 *Spectra before and after de-ghosting (left) averaged over a 5 second window. Narrow-band filtered and 20× gained variable amplitude plots of the stack shown in Figure 5 for 0-5 Hz content (top right) and 34.5-39.5 Hz content (bottom right). Filters had roll-off of 48 dB per octave. Note that a time-varying filter was applied to the full bandwidth data to suppress noise with frequencies above the main signal band. Arrows shown are for the same positions of TB and WB as per Figure 5.*

adaptively for each estimation window. The deghosting process also included a stage of amplitude and phase statistical correction for the minimization of any residual ghost energy. The deghosted, migrated common offset gathers were then stacked. Final processes applied to the data after stack were time-varying filtering, scaling and post-stack deconvolution. The final stack for the example line is shown in Figure 5. The sharp wavelet without side-lobes evidenced in the Figure is typical of the high resolution expected from broadband processing.

Deghosting recovers the original signal level at the interference peaks and notches as evident from the spectrum in Figure 6.

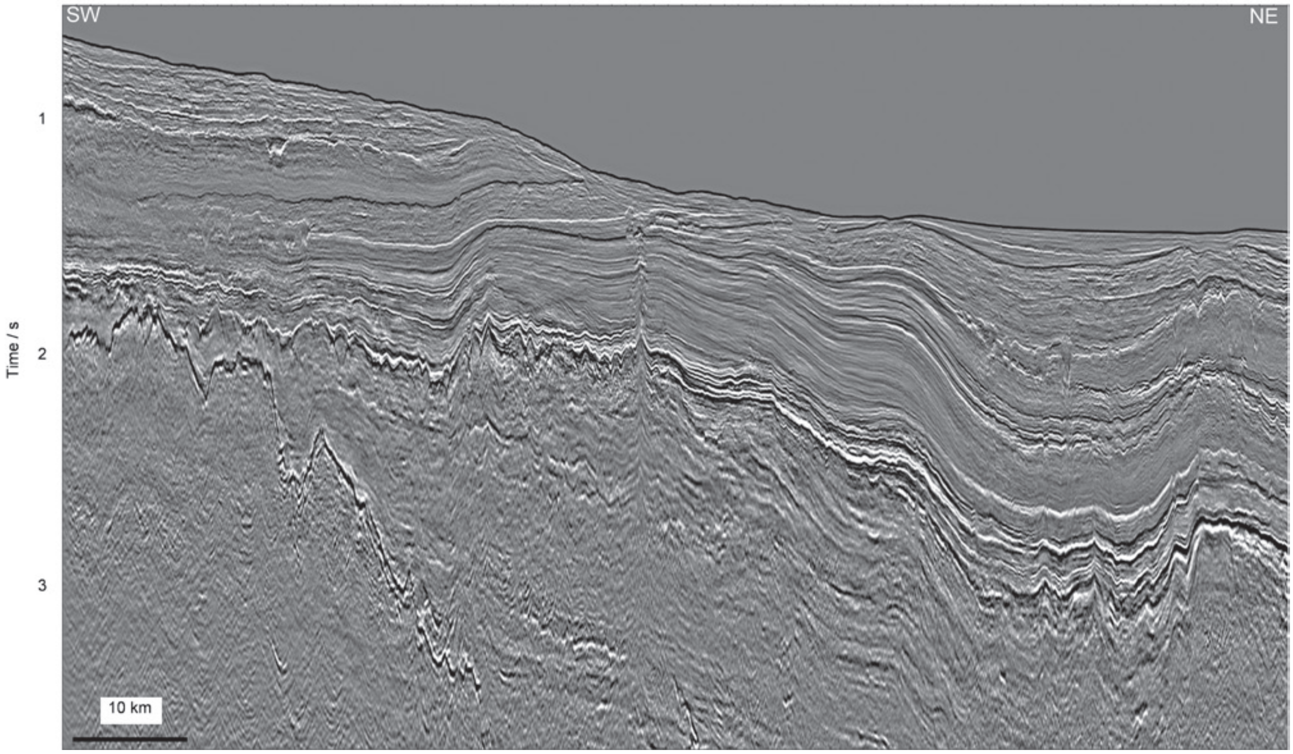

Figure 7 *Close-up of a stacked final section from the southern part of the survey area.*

The good signal-to-noise ratio ensures signal recovery at all frequencies, as evidenced by the narrow-band views of the stacked section at the DC notch frequency 0-5 Hz and centred around the second notch at 37.5 Hz. The low-frequency content shown is of particularly significance; it illuminates the deeper parts of the data including beneath the basalt layer and adds signal level and texture to the overall seismic image that facilitates the interpretation of horizons and subsequent quantitative analyses such as inversion. Figure 7 shows a close-up from another line at the southern end of the survey, again demonstrating the high resolution sidelobe-free wavelet that is achieved, which provides good separation between the many different layers in the shallow and is able to penetrate and maintain high signal-to-noise ratio beneath the basalt.

Discussion

The success of broadband processing requires the removal of ghost events from seismic data. These cause frequency-dependent constructive and destructive interference, with a consequent attenuation of signal in specific frequency bands (notches). Variable depth acquisitions with either a curved or pronounced linear slant provide notch diversity for stacking purposes. However, they induce a strong variability in ghost response with respect to offset, therefore breaking down the stationary wavelet assumption that many processing algorithms require. A more complex, time consuming processing sequence is therefore required (Sablon et al., 2012), or deghosting and re-datuming may be required before demulitple in order to keep the processing sequence simple. On the other hand, when the cable depth is kept constant the processing sequence prior to deghosting does not require modification, and processing turnaround time is not affected.

In the case of constant cable depth acquisitions, deghosting does not rely on notch diversity but on signal-to-noise ratio (SNR), as discussed in Williams and Pollatos (2011). The cable is towed deep for all offsets, therefore guaranteeing a high SNR even at the near offsets, in contrast with slanted or curved acquisitions where these offsets are shallower. Grion et al. (2013) compared broadband images over adjacent lines acquired in calm and rough seas, thus confirming that deep tows and adaptive de-ghosting provide isolation from weather effects for structural imaging purposes. For operational reasons, the cable may be towed with a slight slant (e.g. 1 m per km of offset), which still allows for a conventional pre-deghosting processing sequence.

One of the central benefits of acquiring and processing data in this way is maximizing low-frequency signal content. This ensures a sharper wavelet with minimal sidelobes and enhances the textural information present in the seismic images. It also improves signal-to-noise ratio overall but particularly so in the deeper parts of the data, where low frequency content enables a more effective acoustic impedance inversion to be carried out on the data (Naeini et al., 2014).

Conclusions

Inspection of migrated images and NMO stacks has demonstrated that successful multiple removal could be achieved for a challenging broadband West of Shetland dataset. Algorithms designed for conventional seismic data are therefore confirmed to be suitable for broadband processing, when acquisition is performed using a constant depth deep tow, or with a mild slant. In particular, a shallow-water multiple removal algorithm proved to be more effective than a cascade of SRME and wave-equation demultiple. Particular benefits of the broadband processing of this dataset are a high resolution wavelet and good low-frequency signal content for imaging beneath the basalt. Full-bandwidth stacks and narrow band sections centred on frequencies where ghost destructive interference occurs demonstrate the quality of the obtained results.

Acknowledgements

The data shown are provided courtesy of Dolphin's Multi-Client department.

References

Biersteker, J. [2001] MAGIC: Shell's surface multiple elimination technique. *71st Annual SEG meeting,* Expanded abstracts, 2099-2102.

Grion, S., Azmi, A., Pollatos, J., Riddalls, N. and Williams, R.G. [2013] Broadband processing with calm and rough seas: observations from a North Sea survey. *83rd Annual SEG Meeting,* Expanded Abstracts, 226-230.

Hargreaves, N. [2006]. Surface multiple attenuation in shallow water and the construction of primaries from multiples. *76th Annual SEG Meeting* , Expanded Abstracts, 2689-2693.

Naeini, E., Huntbatch, N., Riddals, N, Zapata, H, Aazmi, A., Telling, R., Grion, S and Williams, R.G. [2014] Broadband processing and inversion of a central North Sea dataset using a deep, flat, hydrophone only cable. *SEG Summer Research Workshop on Broadband Seismic Technology.*

Sablon, R., Russier, R., Hardouin, D., Gratacos, B., Soubaras, R. and Lin, D. [2012] Multiples attenuation for variable depth streamer data, shallow and deep water cases. *74th EAGE Conference & Exhibition*, Extended Abstracts, Y011.

Williams, R.G. and Pollatos, J. [2011] The key to increased marine seismic bandwidth. *First Break*, **30** (11), 101-105.